044 COMBINED STATE AND PARAMETER ESTIMATION OF VEHICLE HANDLING DYNAMICS

Matthew C Best and Timothy J Gordon
Loughborough University, UK

Abstract

This paper considers an extended form of the well-known Kalman filter observer, to reconstruct dynamic states from a small sensor set, but also to rapidly adapt selected parameters in the nonlinear dynamic model which lies at the heart of the observer. A generic procedure is described for constructing the extended Kalman filter in such a way that any combination of model parameters can be identified.

The study is carried out in simulation, using two different vehicle dynamic models, one to act as the test vehicle, the other forming the nucleus of the observer. The assumption is that while in-vehicle testing is most desirable for proving many controller algorithms, here we need 'true' reference state information, to examine Kalman filter accuracy.

A number of experiments are carried out to prove the system's identification properties and also to compare its performance with a more conventional Kalman filter, based on a linear handling model. The results demonstrate high levels of performance and significant robustness to design parameters such as parameter adaptation speed and anticipated sensor noise. Most significantly, the observer also operates well and is capable of parameter adaptation when model and sensor covariance information is not available – usually a restricting factor in practical Kalman filter estimator design. The only significant caveat is that we are 'buying' excellent dynamic tracking from a small sensor set, at some computational expense.

1. Introduction

Recent research has given rise to a number of model-based vehicle control strategies, which rely on suitable low order dynamic models and/or state observers. Methods exist for model identification (eg Best and Gordon, 1999) and also observer design, (eg Kiencke and Daiss, 1997) but research by the authors suggests that the most efficient route to optimal dynamic characterisation is by combining the two processes.

Real-time estimation prescribes a need for low order models, and Kalman filter methods are attractive in exploiting these. However, the performance and optimality of the Kalman filter is fundamentally restricted by model accuracy. Thus the suggested solution for the vehicle handling system is that (a) as complete a model as possible should be incorporated in the filter, and (b) key model parameters should be identified as slow-varying states.

The first requirement leads to the use of a nonlinear model, and hence an extended Kalman filter (EKF). This can be designed in the form :

$$\dot{\hat{\mathbf{x}}} = \mathbf{f}(\hat{\mathbf{x}}, \boldsymbol{\eta}) + \mathbf{K}(\mathbf{s} - \mathbf{h}(\hat{\mathbf{x}}, \boldsymbol{\eta})) \qquad (1)$$

for states $\mathbf{x}$, parameters $\boldsymbol{\eta}$ and sensors $\mathbf{s}$, and where $\mathbf{f}$ and $\mathbf{h}$ are general nonlinear models for the state derivatives and sensors respectively. This structure lends itself to meet the second requirement (b) above, by extension of the state vector to include a subset of parameters $\boldsymbol{\eta}_a$. Although $\mathbf{f}$ is unknown for these parameter states, the expectation is that they will be driven by the second term in equation (1), to improve the innovation error (sensor error, $\mathbf{s} - \mathbf{h}(\hat{\mathbf{x}}, \boldsymbol{\eta})$), provided the optimal feedback matrix $\mathbf{K}$ is suitably formulated. The paper thus prescribes a generic observer/identifier design process which accommodates any choice of $\boldsymbol{\eta}_a$.

In accordance with requirement (a) above, the model has three degrees of freedom and four independent combined-slip Pacejka tyre models; prior experience suggests that the model must include the combined effects of lateral and longitudinal to avoid steady-state parameter estimation errors (see Best and Gordon, 1998). However, these tyre models make the system too complex for real-time estimation, so the emphasis here is to explore the limit of accuracy and flexibility of the new algorithm, rather than provide an immediately realisable observer solution.

The classical Kalman filter combines sensor and model information, using both of these sources to construct a state vector. In this revised structure, variable model parameters cause some shift away from the model as an independently reliable source, but provide a very flexible way of forming a combined observer/identifier whereby both states and parameters are varied to best explain the sensors.

2. Modelling

2.1 Source Model

The study is carried out using a reference source model to provide 'true' state trajectories and sensor measurements. This model simulates full order motion of a rigid vehicle body, with independent suspension freedoms, though 'wheel-hop' modes are suppressed through the assumption of inertia-less wheels. A Pacejka tyre model is implemented in both longitudinal and lateral axes, incorporating a friction limiting ellipse, and the tyre forces have nonlinear load and camber dependent friction. Longitudinal dynamic modes include a simple engine torque model, and road load.

The precise equations for the source model are omitted here, for brevity, but also – as we will see in Section 4.2 – because the detail and even to some extent the accuracy of the source data is of secondary importance; the study should reveal similar results for any suitably formulated high order model, or indeed for an actual test vehicle.

2.2 Observer Model

The observer model is formulated from the popular three degree of freedom yaw/sideslip/roll model, described using vehicle centred SAE axes with roll motion assumed to be constrained about an inclined roll axis (Figure 1). A fourth, longitudinal freedom describes forward speed. The Newton and Euler equations of motion are therefore

for sideslip,

$$M\dot{v} + Mh\dot{p} = \sum_{i=1,4} F_{yi} - Mur \tag{2}$$

for forward speed,

$$M\dot{u} = \sum_{i=1,4} F_{xi} + Mrv + Mhrp \tag{3}$$

for yaw,

$$I_{zz}\dot{r} - I_{xz}\dot{p} = b\sum_{i=1,2} F_{yi} - c\sum_{i=3,4} F_{yi} \tag{4}$$

for roll,

$$\begin{aligned} &-I_{xz}\dot{r} + Mh\dot{v} + I_{xx}\dot{p} = -Mhur - \left(B_f + B_r\right)p + \\ &\left(Mgh - K_f - K_r\right)\phi + \left(h - h_f\right)\sum_{i=1,2} F_{yi} + \left(h - h_r\right)\sum_{i=3,4} F_{yi} \\ &\dot{\theta} = p \end{aligned} \tag{5}$$

Here the forces F_{xi}, F_{yi} acting on the body, are given from tyre forces :

$$\begin{aligned} F_{x1,2} &= F_{tx1,2}\cos\delta - F_{ty1,2}\sin\delta, \qquad F_{x3,4} = F_{tx3,4} \\ F_{y1,2} &= F_{ty1,2}\cos\delta - F_{tx1,2}\sin\delta, \qquad F_{y3,4} = F_{ty3,4} \end{aligned} \tag{6}$$

and the tyre forces are derived using the Pacejka magic formula Ω (see for example Milliken and Milliken, 1995) :

$$F_{txi}, F_{txi} = \Omega_i\left(\frac{C_\alpha \tan\alpha_i}{\mu F_{zi}}, \frac{K_x\left(w - u\cos\alpha_i\right)}{\mu F_{zi}\left(u\cos\alpha_i\right)}, Sp\right) \tag{7}$$

where

$$\begin{aligned} \alpha_1 = \alpha_2 &= \left(\frac{-v - br}{u}\right) + \delta \\ \alpha_3 = \alpha_4 &= \left(\frac{rc - v}{u}\right) \end{aligned} \tag{8}$$

Vertical load transfer due to roll is then included by

$$\begin{aligned} F_{z1,2} &= \frac{cmg}{2(b+c)} \pm \left(F_{y1,2}h_{rf} - K_f\theta - B_f p\right) \\ F_{z3,4} &= \frac{bmg}{2(b+c)} \pm \left(F_{y3,4}h_{rr} - K_r\theta - B_r p\right) \end{aligned} \tag{9}$$

The observer model is therefore completely described in terms of five state variables, 23 constant parameters, and two inputs, summarised in Table 1.

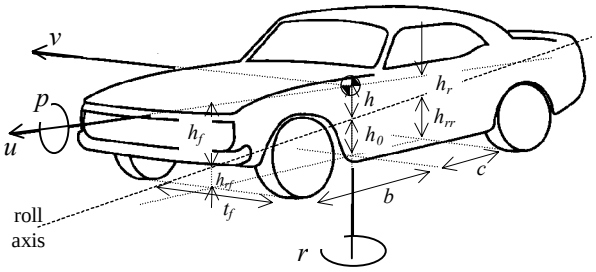

Figure 1 : *Kalman filter model axis system and roll axis geometry*

The Kalman filter is required to estimate the five states, and adapt a number of the parameters to most accurately describe the variation of a set of sensors. These must therefore fully represent the vehicle dynamics, and although rate sensors are included for some experiments, the basic sensor set is made up of four accelerometers. These are oriented in two pairs, one pair above the front axle at a height h_{fs}=0.3m above the roll axis, the other above the rear axle at h_{rs}=0.5m. Within each pair, the first sensor is aligned longitudinally and the second laterally. They are modelled as

$$\begin{aligned} s_1 &= \dot{u} - r\left(v + h_{fs}p\right) + \varepsilon_1 \\ s_2 &= \dot{v} + h_{fs}\dot{p} + b\dot{r} + ru + \varepsilon_2 \\ s_3 &= \dot{u} - r\left(v + h_{rs}p\right) + \varepsilon_3 \\ s_4 &= \dot{v} + h_{rs}\dot{p} - c\dot{r} + ru + \varepsilon_4 \end{aligned} \tag{10}$$

Unmodelled measurement noise is simulated using an independent Gaussian white noise signal with equal magnitude on each sensor :

$$\varepsilon_i \propto N\left(0,\left[8\rho\right]^2\right) \tag{11}$$

where ρ = 0.2. Thus the RMS noise can be interpreted as 20% of a relatively high lateral acceleration of 8m/s^2.

States, $\boldsymbol{x}$	
u	forward velocity (*m/s*)
v	sideslip velocity (*m/s*)
p	roll angular velocity (*rad/s*)
r	yaw angular velocity (*rad/s*)
θ	roll angle (*rad*)
parameters, $\boldsymbol{\eta}$ (*default values*)	
I_{xx}	roll moment of inertia (*600 kgm^2*)
I_{zz}	yaw moment of inertia (*1300 kgm^2*)
I_{xz}	roll/yaw cross moment of inertia (*80 kgm^2*)
m	mass (*830 kg*)
b	longitudinal Distance of C of G to front axle (*1.1 m*)
c	longitudinal Distance of C of G to rear axle (*1.4 m*)
h	C of G height above roll axis (*0.347 m*)
h_0	ground plane to roll axis distance below CofG (*0.3 m*)
h_f	roll axis to x axis vert. distance at front axle (*0.45 m*)
h_r	roll axis to x axis vert. distance at rear axle (*0.25 m*)
t_f	front track (*1.5 m*)
t_r	rear track (*1.5 m*)
K_f	front roll stiffness (*34 kNm/rad*)
K_r	rear roll stiffness (*22.5 kNm/rad*)
B_f	front roll damping (*1700 Nms/rad*)
B_r	rear roll damping (*1700 Nms/rad*)
Sp	Pacejka tyre model shape coefficients (*0.714, 1.4, 1.0, -0.2*)
C_α	zero lateral slip cornering stiffness (*35 kN*)
K_x	zero longitudinal tyre slip rate (*35 kN*)
μ	tyre friction coefficient (*1.0*)
Inputs, $\boldsymbol{u}$	
δ	front wheel steer angle (*rad*)
w	front wheel speed referenced to forward speed (wheel angular velocity multiplied by rolling radius, *m/s*)

Table 1 : *Model nomenclature*

3. Formulation of Kalman Filters

3.1 Linear Kalman Filter

As a basis for evaluating the extended Kalman filter we first derive the equivalent linear time-invariant form. The linear model is formed from equations (2),(4) and (5) for the reduced state vector $\mathbf{z} = \left[r,v,p,\phi\right]^{\mathbf{T}}$, with u assumed constant and replacing the nonlinear tyre model with linear (cornering stiffness) multipliers of α from equation (8). Exponential discretisation of these linear equations then gives a model **A**, **B**, **C**, **D** which can be related to the *'true' source states* $\mathbf{z}^{\mathbf{s}}$ by

$$\begin{aligned} \mathbf{z}^s_{k+1} &= \mathbf{A}\mathbf{z}^s_k + \mathbf{B}\delta_k + \boldsymbol{\omega}_k \\ \mathbf{y}_k &= \mathbf{C}\mathbf{z}^s_k + \mathbf{D}\delta_k + \boldsymbol{\upsilon}_k \end{aligned} \tag{12}$$

Here process and measurement errors are denoted $\boldsymbol{\omega}_k$ and $\boldsymbol{\upsilon}_k$ respectively, and an optimal filter can easily be derived, provided the following expectations $E(\ )$ apply:

$$E\left(\boldsymbol{\omega}_k\right) = \mathbf{0}, \qquad E\left(\boldsymbol{\upsilon}_k\right) = \mathbf{0}, \qquad \forall k$$

$$E\left(\boldsymbol{\omega}_i\boldsymbol{\omega}_j^T\right) = \mathbf{0}, \qquad E\left(\boldsymbol{\upsilon}_i\boldsymbol{\upsilon}_j^T\right) = \mathbf{0}, \qquad \forall\left(i \neq j\right)$$

The simplest form of the Kalman filter also assumes $E\left(\boldsymbol{\omega}_k\boldsymbol{\upsilon}_k^T\right) = \mathbf{0}$, $\forall k$ but this can not be expected here; for accelerometers the sensor model **C**, **D** correlates with **A**, **B**, and this ensures that $\boldsymbol{\omega}_k$ and $\boldsymbol{\upsilon}_k$ share a common modelling error component. The Kalman filter is thus specified in the more general form (eg from Gelb, 1974),

$$\hat{\mathbf{z}}_{k+1} = \left(\mathbf{A}-\mathbf{K}\mathbf{C}\right)\hat{\mathbf{z}}_k + \left(\mathbf{B}-\mathbf{K}\mathbf{D}\right)\delta_k + \mathbf{K}\mathbf{y}_k \tag{13}$$

with the (time-invariant) gain matrix **K** found through calculation of the anticipated state error covariance matrix **P**, which is the solution to the algebraic Riccati equation :

$$\begin{aligned} \mathbf{P} &= \mathbf{G}\mathbf{P}\mathbf{G}^{\mathbf{T}} - \mathbf{G}\mathbf{P}\mathbf{C}^{\mathbf{T}}\left[\mathbf{C}\mathbf{P}\mathbf{C}^{\mathbf{T}} + \mathbf{R}\right]^{-1}\mathbf{C}\mathbf{P}\mathbf{G}^{\mathbf{T}} + \overline{\mathbf{Q}} \\ \mathbf{K} &= \left(\mathbf{A}\mathbf{P}\mathbf{C}^{\mathbf{T}} + \mathbf{S}\right)\left(\mathbf{C}\mathbf{P}\mathbf{C}^{\mathbf{T}} + \mathbf{R}\right)^{-1} \end{aligned} \tag{14}$$

where

$$\begin{aligned} \mathbf{G} &= \mathbf{A} - \mathbf{S}\mathbf{R}^{-1}\mathbf{C} \\ \overline{\mathbf{Q}} &= \mathbf{Q} - \mathbf{S}\mathbf{R}^{-1}\mathbf{S}^{\mathbf{T}} \end{aligned} \tag{15}$$

and

$$\mathbf{e}_k = \begin{bmatrix} \boldsymbol{\omega}_k \\ \boldsymbol{\upsilon}_k \end{bmatrix}, \quad E\left(\mathbf{e}_k\mathbf{e}_k^{\mathbf{T}}\right) = \begin{bmatrix} \mathbf{Q} & \mathbf{S} \\ \mathbf{S}^{\mathbf{T}} & \mathbf{R} \end{bmatrix} \tag{16}$$

3.2 Extended Kalman Filter

The extended filter employs the fully nonlinear model of equations (2) – (10), which can be written for continuous state propagation, and sampled sensor data in the general form,

$$\begin{aligned} \dot{\mathbf{x}}^s(t) &= \mathbf{f}\left(\mathbf{x}^s(t),\boldsymbol{\eta},\mathbf{u}(t)\right) + \boldsymbol{\omega}(t) \\ \mathbf{y}_k &= \mathbf{h}\left(\mathbf{x}^s_k,\boldsymbol{\eta},\mathbf{u}(t)\right) + \boldsymbol{\upsilon}_k \end{aligned} \tag{17}$$

Gelb (1974) propose estimation of $\hat{\mathbf{x}}$ by the use of a truncated Taylor series for $\mathbf{f}\left(\mathbf{x}(t)\right)$ in the continuous model and state error covariance matrix estimate. The observer is then derived in a continuous-discrete form, using continuous model propagation combined with sampled measurements which provide discrete state

corrections. The final form is then fully discretised to a practicable form.

Assuming time-invariant noise covariance matrices, and again incorporating the general form for correlated model and sensor errors, (which is expounded in Best et al, 2000) the resulting algorithm provides the following models for state and state error covariance matrix derivatives :

$$\begin{aligned}\dot{\hat{\mathbf{x}}}(t) &= \mathbf{f}(\hat{\mathbf{x}}(t), \eta, u) \\ \dot{\mathbf{P}}(t) &= \mathbf{G}(t)\mathbf{P}(t) + \mathbf{P}(t)\mathbf{G}^{\mathrm{T}}(t) + \overline{\mathbf{Q}}\end{aligned} \tag{18}$$

where

$$\begin{aligned}\mathbf{G}(t) &= \mathbf{F}(t) - \mathbf{S}\mathbf{R}^{-1}\mathbf{H}(t) \\ \overline{\mathbf{Q}} &= \mathbf{Q} - \mathbf{S}\mathbf{R}^{-1}\mathbf{S}^{\mathrm{T}}\end{aligned}$$

and the sensors provide filter and state corrections at each discrete time step, to improve the variable estimates from the (-) to (+) form :

$$\begin{aligned}\hat{\mathbf{x}}_k(+) &= \hat{\mathbf{x}}_k(-) + \mathbf{K}_k\left[\mathbf{y}_k - \mathbf{h}(\hat{\mathbf{x}}_k(-), \eta, u)\right] \\ \mathbf{P}_k(+) &= \left[\mathbf{I} - \mathbf{K}_k\mathbf{H}(\hat{\mathbf{x}}_k(-))\right]\mathbf{P}_k(-)\end{aligned} \tag{19}$$

where

$$\mathbf{K}_k = \mathbf{P}_k(-)\mathbf{H}^{\mathrm{T}}(\hat{\mathbf{x}}_k(-))\left[\mathbf{H}(\hat{\mathbf{x}}_k(-))\mathbf{P}_k(-)\mathbf{H}^{\mathrm{T}}(\hat{\mathbf{x}}_k(-)) + \mathbf{R}\right]^{-1}$$

In the above, matrices **F** and **H** are Jacobians resulting from the Taylor series expansions, evaluated at the state estimates :

$$\begin{aligned}\mathbf{F}(t) &= \left.\frac{\partial \mathbf{f}(\mathbf{x}(t), \eta, u(t))}{\partial \mathbf{x}(t)}\right|_{\mathbf{x}(t)=\hat{\mathbf{x}}(t)} \\ \mathbf{H}(t) &= \left.\frac{\partial \mathbf{h}(\mathbf{x}(t), \eta, u(t))}{\partial \mathbf{x}(t)}\right|_{\mathbf{x}(t)=\hat{\mathbf{x}}(t)}\end{aligned} \tag{20}$$

These equations constitute the complete extended Kalman filter in a continuous form, with discrete sensor correction. Provided a suitably low sampling interval T is chosen, the discrete state update can be approximated from equations (18) by Euler integration

$$\hat{\mathbf{x}}_{\mathbf{k+1}} = \hat{\mathbf{x}}_{\mathbf{k}} + T\dot{\hat{\mathbf{x}}}(t), \qquad \mathbf{P}_{\mathbf{k+1}} = \mathbf{P}_{\mathbf{k}} + T\dot{\mathbf{P}}(t) \tag{21}$$

It should be noted at this point that **F**(t) and **H**(t) would normally be described analytically, and indeed these derivatives can theoretically be derived for the model used here, but the tyre nonlinearities make the resultant formulae particularly complex. In practice, equation (20) is evaluated numerically, within the state update loop, by re-evaluating ***f*** and ***h*** for small changes in each of the five states.

3.3 Adapting Model Parameters

Given the general form for $\mathbf{f}(\mathbf{x}(t))$, the model can readily be specified in terms of an extended state vector $\boldsymbol{\chi}$(t), to include any number of the parameters :

$$\dot{\boldsymbol{\chi}}(t) = \begin{bmatrix}\dot{\mathbf{x}}^s(t) \\ \dot{\boldsymbol{\eta}}_a(t)\end{bmatrix} = \begin{bmatrix}\mathbf{f}\left(\mathbf{x}^s(t), \boldsymbol{\eta}, \mathbf{u}(t)\right) \\ \mathbf{f}_a\left(\mathbf{x}^s(t), \boldsymbol{\eta}, \mathbf{u}(t)\right)\end{bmatrix} + \begin{bmatrix}\boldsymbol{\omega}(t) \\ \boldsymbol{\omega}_a(t)\end{bmatrix} \tag{22}$$

If the original model is valid, all the parameters are time invariant, so $\mathbf{f}_a\left(\mathbf{x}(t), \boldsymbol{\eta}, \mathbf{u}(t)\right) = 0$ and the rate of change of these parameter states is given by $\boldsymbol{\omega}_a$ (t). The new model error covariance and model/sensor cross covariance matrices become

$$\mathbf{Q}_\chi = \begin{bmatrix}\mathbf{Q} & E(\boldsymbol{\omega}\boldsymbol{\omega}_{\mathbf{a}}^{\mathbf{T}}) \\ E(\boldsymbol{\omega}_{\mathbf{a}}\boldsymbol{\omega}^T) & E(\boldsymbol{\omega}_{\mathbf{a}}\boldsymbol{\omega}_{\mathbf{a}}^{\mathbf{T}})\end{bmatrix}, \quad \mathbf{S}_\chi = \begin{bmatrix}\mathbf{S} \\ E(\boldsymbol{\omega}_{\mathbf{a}}\boldsymbol{\upsilon}^T)\end{bmatrix} \tag{23}$$

4. Simulation Experiments

4.1 Design Process

For all the simulation experiments, error covariance matrices **Q**, **R** and **S** are estimated from a single reference simulation, designed to excite the system at high amplitude, over a range of frequencies. The throttle and steer inputs for the source model are illustrated for this 15 second test in Figure 2, along with the wheel velocity output from the source model, which is used as an input to the estimator (w). The test is designed to be achievable in a real vehicle, so the random steer and throttle sections are generated using white noise which is bandlimited within a physically realisable range, to 5Hz.

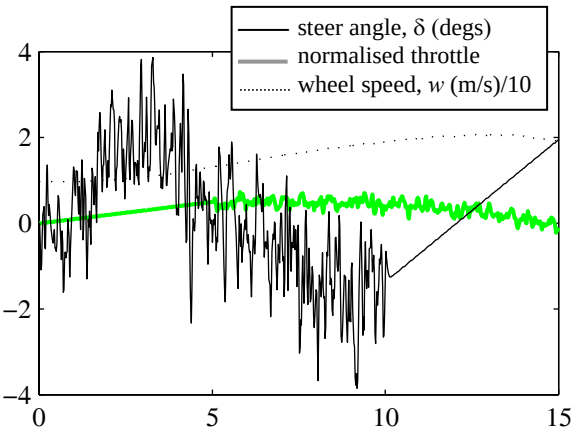

Figure 2 : *Test inputs for noise matrix identification*

Equations (12) and (17) are applied to the simulation results to establish time histories for **ω** and **υ**, and **Q**, **R** and **S** are then formed separately for the linear and extended Kalman filters, in an obvious way, from equation (16). The observers are tested on independent test inputs, with a sampling interval T = 0.02 secs.

4.2 Non-adaptive Observers

Performance is first examined with no parameter adaptation ($\boldsymbol{\eta}_a = \mathbf{0}$), for a δ = 4° step steer, with zero throttle input, at 18m/s (Figure 3). The plots show source

model time histories against results for both designs of Kalman filter and also traces from the Kalman filter model simulated without sensor feedback, for this five second test.

The linear Kalman filter estimates are poor for this fairly severe steer input. The assumption that both speed and cornering stiffness are constant, causes large errors which are particularly evident in plot (b) for sideslip, and in the tracking of lateral accelerations – plot (f).

With the nonlinear model, the EKF is more accurate in s_2, r and for much of the test, in v. These results are good in spite of the very high, although realistic, noise levels which have been imposed on the sensors. Also note the dotted line time histories, which show that large steady-state differences exist between the EKF and source models; all of the EKF results might be improved by suitable parameter identification in its model.

One immediate benefit of EKF over the linear filter is illustrated in plot (g); vertical load is an intermediate variable in the EKF model. Although steady-state errors are again seen in this prediction, the ability of EKF to estimate values such as this leads to a more complete dynamic characterisation of the vehicle.

Conversely, the algorithm also presents a poor result in its reconstruction of roll rate – plot (c). This problem, also seen in earlier studies (see Best et al, 2000) is caused by the structural difference between source and EKF roll models, causing large expected model errors for p in the **Q** matrix, and hence allowing greater transmission of sensor noise into the state estimate.

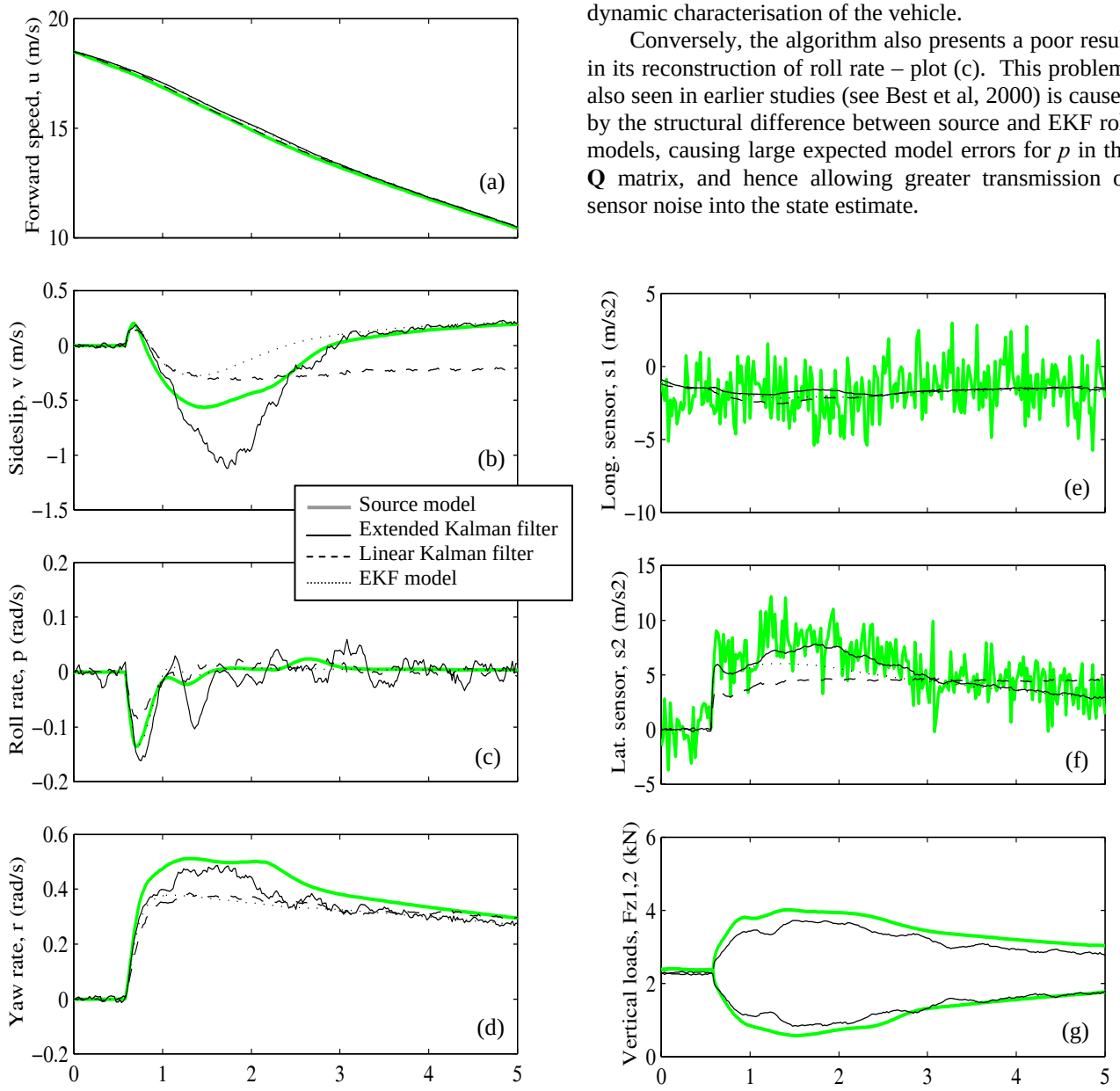

Figure 3 : *Non-adaptive observer results*

These errors can be reduced by increasing the EKF model order further, but significant improvement can also be achieved through the addition of a roll rate sensor, as we will see in Section 4.4.

4.3 Introducing Parameter Adaptation

A significant error from the EKF in Figure 3 is the overestimation of peak sideslip. This is caused by errors in the slip to tyre force relationship, so could be improved by modifying the tyre model; an obvious

candidate for adaptation is the base cornering stiffness on which the Pacejka model depends : C_α.

In extending the EKF to include parameter states however, we first need to provide an estimate for the additional error matrix components in equation (23). This is done by adding band-limited white noise to the parameters $\boldsymbol{\eta}_a$ during the reference simulation described in Section 4.1, such that

$$\boldsymbol{\eta}_a(t) = \boldsymbol{\eta}_a + \boldsymbol{\varepsilon}_a(t)$$

where for the i^{th} parameter state,

$$\varepsilon_{a(i)} \propto N\left(0, \lambda \eta_{a(i)}\right)$$

An estimate for $\boldsymbol{\omega}_a(t)$ can then be found by suitably accurate numerical differentiation, as $\boldsymbol{\omega}_a(t) = \dot{\boldsymbol{\varepsilon}}_a(t)$ from equation (22); this explains the need for some band-limitation on $\boldsymbol{\varepsilon}_a$, and for these experiments a limit of 5Hz was used. Matrices $\mathbf{Q}_\chi$ and $\mathbf{S}_\chi$ are constructed again from equation (16), now using $\mathbf{e}_k = [\boldsymbol{\omega}_k, \boldsymbol{\omega}_{ak}, \boldsymbol{\upsilon}_k]$.

Figure 4 shows the adapted cornering stiffness, along with the new EKF prediction for v when the step steer test is repeated. The adaptation of C_α is caused by, and acts to reduce the near steady-state errors in s_2 which

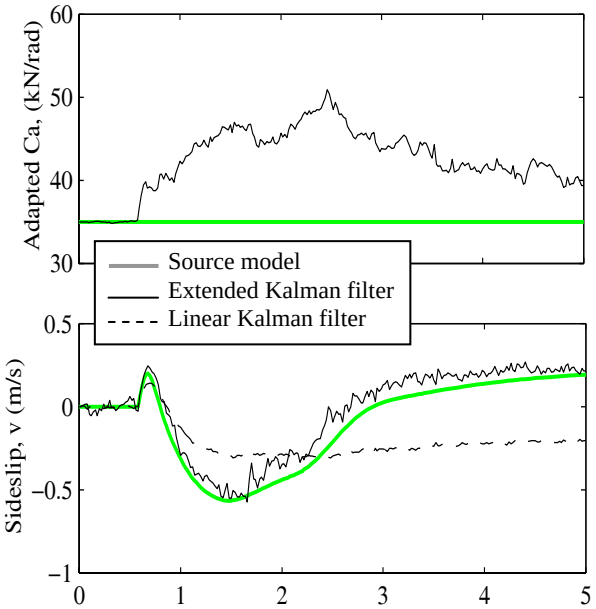

Figure 4 : *EKF results for an observer with Cα estimation*

can be seen after the step between 0.5 and 2 seconds in Figure 3(f). The result is a large improvement in estimation of v.

This is an excellent result, but the accuracy of v turns out to be sensitive to the choice of λ, which was set arbitrarily to 0.2 here. Also, the adaptation is triggered here by an impulsive input which causes little dynamic excitation in the sensors that drive the adaptation process. The conclusion is that adaptation would be more robust under continuous dynamic excitation.

4.4 Parameter Identification

With a dynamic input, EKF is capable of simultaneously adapting multiple parameters. Here we consider estimation of the x and z axis locations of the vehicle's centre of gravity, so $\boldsymbol{\eta}_a = [h, b]$. A 5Hz band-limited Gaussian signal is again used for the steer input – here with an RMS of 1.5° – and a constant 75Nm engine torque is applied. $\boldsymbol{\eta}_a$ is then initialised to inappropriate values, [0.7, 0.2], and Figure 5 shows the adaptation for a range of choices of λ.

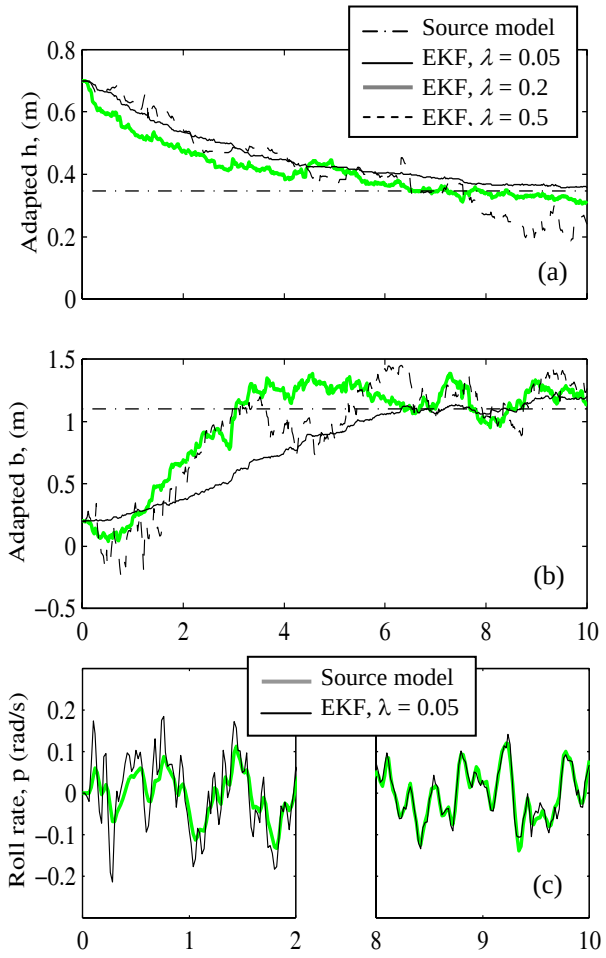

Figure 5 : *EKF results for C of G identification*

The conclusion is that adaptation works very well, and rapidly under these conditions. The process is also robust to variation of λ, with a positive correlation between speed of response and λ, and also between standard deviation of the adapted parameters, and λ. This might reasonably be expected, given the influence that λ has setting the relative balance between expected sensor and model ($\mathbf{f}_a = \mathbf{0}$) accuracy in the observer design process; higher λ promotes a greater magnitude of sensor feedback.

Figure 5(c) gives an example of how the tuned parameters also improve state prediction – showing the first and last two seconds of the estimation of *p*. In this test we have included an additional roll sensor – although this was not necessary to achieve correct adaptation of *h* and *b*. The additional sensor generally improves roll prediction compared with the Figure 3 result, and we also see roll accuracy improve with time, as *h* and *b* adapt.

4.5 Noise Matrix Dependence

As it has been described and used so far, the adaptive EKF could be applied to predict the response of a real vehicle (albeit not in real-time), *except* in that we have assumed detailed *a priori* knowledge of the error correlations in **Q**, **R** and **S**. In practice these are very difficult to obtain, so EKF performance under nominal noise matrices is also of interest.

The centre of gravity experiment is therefore repeated, this time with **Q** and **R** determined as diagonal matrices simply proportional to expected state and sensor RMS amplitude on the noise identification test, and with **S** = **0**.

$$Q_{i,i} = \lambda_{\text{mod}}\left(\bar{\omega}_i^2\right), \qquad i = 1,5$$

$$Q_{i,i} = \left(\bar{\omega}_{a(i-5)}^2\right), \qquad i > 5$$

$$R_{j,j} = \lambda_{\text{mod}}\left(\bar{\upsilon}_i^2\right), \qquad j = 1,5$$

Considering two alternatives for the new nominal error factor λ_{mod}, and again using $\lambda = 0.2$, the adaptation result is compared with the standard **Q**,**R**,**S** result in Figure 6. (For all three results we have reverted here to the standard four accelerometer sensor set.)

Remarkably, the nominal noise settings also induce good adaptation of centre of gravity, with no difference in the overall estimate for *b*, and only slight variation for *h* – also the success of adaptation itself is not sensitive to λ_{mod}.

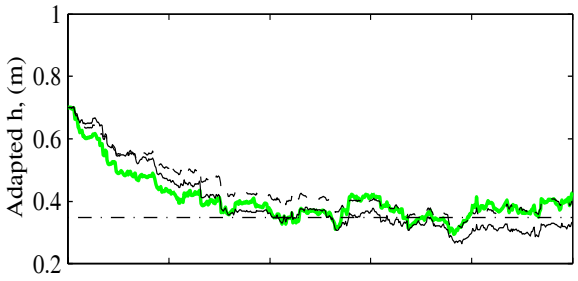

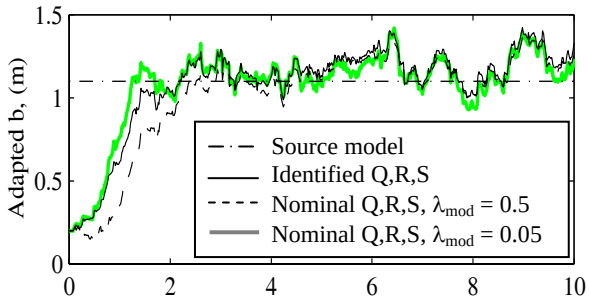

Figure 6 : *Comparing nominal with correlated noise matrices for an EKF with C of G identification*

For this experiment, accuracy in prediction of the states and sensors is summarised in terms of RMS errors in Table 2. Here we see that errors in estimating the sensors are reduced by increasing the adaptation rate. (Under this EKF design, it is the lower setting, λ_{mod} = 0.05 which generates faster adaptation, because expected sensor modelling errors are lower.) Critically, an improvement in state reconstruction is also seen as the sensor model improves. Note that the best nominal test provides RMS errors which are even lower than for the standard **Q**,**R** and **S**. This is a happy consequence of low noise expectation, and we are comparing filters with quite different assumptions, but the result is nevertheless encouraging.

QRS → state/sensor	Nominal, λ_{mod} = 0.5	Nominal, λ_{mod} = 0.05	Identified
u	.1252	.1189	.1180
v	.0440	.0333	.0461
p	.0510	.0274	.0447
r	.0336	.0184	.0241
q	.0060	.0029	.0044
s_1	.2814	.0813	.0827
s_2	.8295	.7401	.7863
s_3	.2842	.0795	.0811
s_4	.8539	.4884	.7628

Table 2 : *Comparing state and sensor RMS errors during adaptation under nominal and standard noise matrices.*

4.6 Multi-parameter Optimisation

As a final investigation of the potential of the new algorithm, we consider increasing the number of identified parameters. This is only feasible if a larger number of sensors is also considered, as clearly there is scope for the algorithm to become poorly conditioned, and hence unstable, so here we have augmented the set of four accelerometers with roll and yaw rate sensors.

Figure 7 demonstrates simultaneous estimation of mass, roll inertia, yaw inertia and longitudinal mass centre position – certainly an ambitious venture, with all

four parameters initialised to ridiculously low values, $\boldsymbol{\eta}_a(0) = [100, 100, 100, 0.5]$

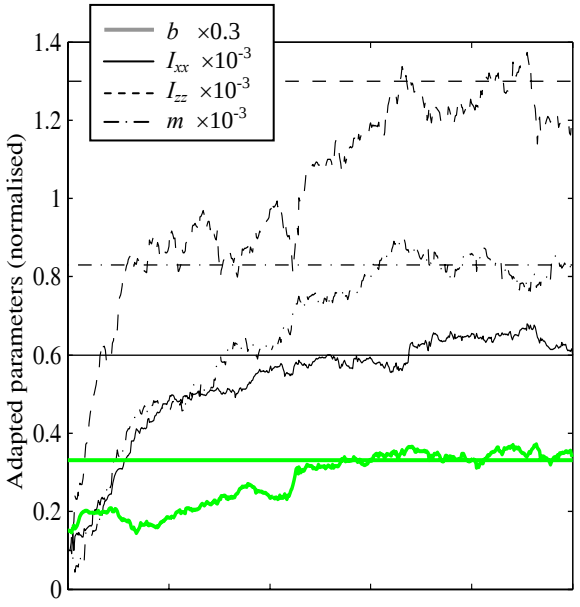

Figure 7 : An *example of multi-parameter identification using EKF*

The results are impressive, and it is interesting to see that the parameters are adapting at different rates through the ten second test. I_{zz} and b also appear to temporarily settle at intermediate values – possibly local minima – up to about four seconds.

One disappointing footnote however, is that no suitable value for λ_{mod} could be found to make this adaptation work with nominal noise matrices – a point which does serve to emphasise the importance of error expectations in this multi-dimensional process.

Concluding Remarks

The new observer / identifier works well within the simulation environment considered here, and its robustness to design parameter variations makes success in real-vehicle applications likely. Some good results with nominal noise matrices also improve the likelihood of practical viability, especially if these too are adapted – methods exist in Gelb (1974).

Long computer processing times make on-line application impossible given the model structure used here, but the system still has scope for immediate application in off-line state and parameter reconstruction – for example to assist vehicle design in the motorsport field. The most likely future for on-line development is by selective model reduction – for example by consolidating the tyre force model to a simple generic nonlinear load-dependent function of a small number of parameters.

References

1. Best M.C. and Gordon T.J. (1999), "A Randomised Integral Error Criterion for Parametric Identification of Dynamic Models of Mechanical Systems" *IMechE Journal of Systems and Control Engineering (Part I),* Vol 213, pp 119-134.
2. Kiencke, U. and Daiss, A. (1997), "Observation of Lateral Vehicle Dynamics" *Control Engineering Practice,* Vol 5, No 8, pp 1145-1150.
3. Best M.C. and Gordon T.J. (1998), "Real-Time State Estimation of Vehicle Handling Dynamics Using an Adaptive Kalman Filter" *proceedings from the 4th International Symposium on Advanced Vehicle Control (AVEC),* Nagoya, Japan, September 1998, pp 183-188.
4. Milliken W.F. and Milliken D.L. (1995), "Race Car Vehicle Dynamics" *SAE International.*
5. Gelb, A. (1974), "Applied Optimal Estimation", *MIT Press*, Cambridge Mass.
6. Best M.C., Gordon T.J. and Dixon P.J. (2000), "An Extended Adaptive Kalman Filter for Real-time State Estimation of Vehicle Handling Dynamics" *Vehicle System Dynamics* (accepted for publication Dec 1999).